PROBLEMS OF MECHATRONICS
ARMAMENT, AVIATION, SAFETY ENGINEERING

ISSN 2081-5891

4, 2 (12), 2013, 19-30

Building and Validation of Numerical Models of the B-32 Type Armour-Piercing Projectiles*

Adam WIŚNIEWSKI, Paweł ŻOCHOWSKI

Military Institute of Armament Technology, 7 Wyszyńskiego St., 05-220 Zielonka, Poland

Abstract. Process of building and the validation of the numerical models of the B-32 type armour-piercing incendiary (API) projectile is described in this article. Results of projectile compression tests (static and under high strain rates with the use of the modified Split Hopkinson Pressure Bar) are shown. On the basis of this, the values of the Johnson–Cook (J–C) strength model parameters for the projectile core material (N12e steel) were determined. This article presents results gained from simulations of the tests, in which the B-32 type projectile was modelled with the use of determined values of the J–C strength and failure models parameters. The process of the parameters values verification was described, in which the stress and strain obtained from samples in experiments and simulations were compared. Additional verification of the determined parameters values was comparison to the depth of penetration (*DP*) tests results of the Armox 500T plates fired with the 12.7 mm B-32 type projectile, obtained experimentally and in simulations. Small differences (< 5%) between stress and penetration depths obtained in the simulations and in the tests showed that the J–C parameter values were determined correctly.

Keywords: mechanics, terminal ballistics, numerical simulations of penetration, penetration of steel, API projectile

* This paper is based on the work presented at the 9th International Armament Conference on „Scientific Aspects of Armament and Safety Technology", Pułtusk, Poland, September 25-28, 2012

1. INTRODUCTION

Numerical simulations are a popular and commonly applied tool for the analysis of complex dynamic physical phenomena in high strain rate conditions.

Widely available commercial computer hydro-codes (LS-Dyna, Autodyn) can simulate a bodies behaviour in different load conditions, thanks to the use of different techniques of calculations. These programs allow observations of dynamic phenomena (strain or stress changes in the material in every moment of simulation etc.), accurate analysis of which is difficult or impossible during tests.

The use of numerical methods in initial stages of armour designing processes allows us to evaluate the effectiveness of a developed construction, without the necessity of building and conducting firing tests. It significantly reduces costs and time needed for the construction of new types of armours.

To obtain simulation results which are concurrent with test results, reliable and accurate material models of armour and projectiles must be used to prepare the simulation. The building of the correct numerical model for the given material requires the determination of values of several parameters (material constants) in the materials equations of state, strength and failure models.

Many of these parameters show dynamic characteristics, i.e. they change depending on the strain rate. Therefore, in order to determine these values it is necessary to conduct expensive and accurate strength tests, both static and dynamic. The building process of the B-32 type API projectiles (7.62 mm, 12.7 mm, 14.5 mm) numerical models, which are made of the same materials, are described in this article (Fig. 1).

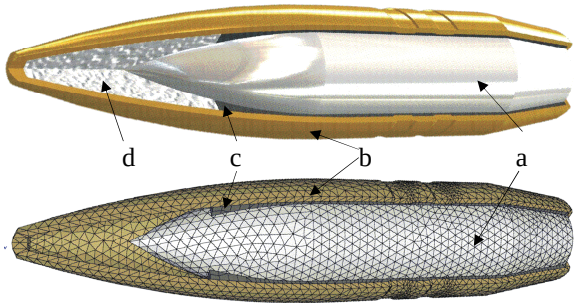

Fig. 1. B-32 type API projectile:
a – steel core, b – tombac plated steel jacket,
c – lead can, d – incendiary material

The authors focused on B-32 API projectile core material (N12e steel) which has the biggest influence on its high rate of effective. Knowledge of this materials properties is essential because B-32 type projectiles determines the protection levels according to the international agreement STANAG 4569

(7.62 mm projectile – 3 level STANAG, 12.7 mm projectile – 3+ level STANAG, 14.5 mm projectile – 4 level STANAG). The protection class is given to armour based on its resistance to these projectiles.

In the future projectiles material models built on the basis of material constants obtained from tests, will be used to numerically calculate new armour constructions.

2. RESEARCH PROGRAMME

For the purpose of building and validation of the B-32 type projectiles numerical models of the following tests were performed:

1. static uniaxial compression;
2. compression under high strain rates with the use of the modified Split Hopkinson Pressure Bar;
3. *DP* tests of three coherent Armox 500T plates, fired with the 12.7 mm type B-32 projectile.

Stress-strain curves obtained as a result of carried out experimental tests allow the determination of the N12e steels mechanical parameter values (elastic constants) and the J-C model material constants. These values were used to make simulations of tests. Based on the comparisons of character and values of samples stress and strain, obtained in simulations from the experimental results, the values of the failure model constants were also determined. Verification of the numerical models was made by comparisons of the *DP* with three coherent Armox 500T plates, fired with a 12.7 mm type B-32 projectile, obtained experimentally and in simulations.

2.1. Test equipment

Static uniaxial compression tests were carried out on the universal material testing machine Instron 8802 with Fast Track control software (Fig. 2a). During tests, to measure the longitudinal and transverse strain, strain rosettes and a bridge were used. The strain measurements with the rosettes were carried out to obtain the value of the longitudinal strain of 0.05 and transverse strain of 0.025. During static compressive tests, to strain measurement the longitudinal extensometer with the 12.5 mm measuring base and the ± 5 mm range was used. Measured signals were converted by a computer with special extensometer software (Fig. 2b).

Compression tests under high strain rates were made with the use of the modified Split Hopkinson Pressure Bar stand. The Tasler LTT 500 preamplifier and the NOR USB-6366 measuring card were used to amplify signals from measuring bars. The test stand with its equipment is shown in Figure 3.

Fig. 2. Static compression test stand:
a – Instron 8802 material testing machine,
b – extensometric testing equipment to strain measurement

Fig. 3. High strain rates test stand:
a – system of the Split Hopkinson Pressure Bars,
b – computer system of the testing stand control

Armox 500T plates *DP* tests were carried out on the range of the Military Institute of Armament Technology in Zielonka. Three Armox 500T steel plates of $500 \times 500 \times 10$ mm dimensions were screwed into a special frame. Elements of the *DP* testing stand and the projectile used in the firing are shown in Figure 4.

Fig. 4. The frame to fix the Armox 500T plates (a), *DP* testing stand (b), DSZK rifle (c), 12.7 mm cartridge with the B-32 type API projectile (d)

Samples for tests were prepared using projectiles cores, obtained first by disassembling projectiles into elements. Next, cylinders of D = 8 mm diameter were turned from the cores, then cut and grinded to achieve samples of L = 12 mm length to static tests, and of L = 8 mm length to high strain rates tests. The method of preparing samples from the cores is shown in Figure 5a. One sample of L = 12 mm length and two samples of L = 8 mm length were prepared from each core. The strain rosettes were stuck onto the ready samples and the cables were soldered. The set of samples prepared for tests is shown in Figure 5b.

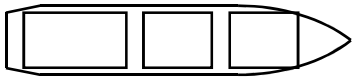

a

b

Fig. 5. Samples for compression tests: a – the shape and way of samples preparation, b – the samples with the stuck on strain rosettes, ready to tests

3. TESTS

The static compression tests were carried out on the Instron 8802 material testing machine with the controlled force increment ratio of 120 kN per minute. During tests the following parameters were registered: displacement of the testing machine jaws, force, strain of sample with the use of extensometer; longitudinal and transverse strains with the use of the strain rosette. The tests were concluded upon the destruction of samples. In Figure 6 the sample installed in the testing machine before the test and several samples after the tests are shown.

Additional disks of diameters equal to test bars and of 10 mm thickness (Fig. 7) were used in the tests at high strain rates due to the hardness of steel (> 60 HRC).

a

b

Fig. 6. Samples for compression tests:
a – in jaws of the mechanical testing machine, b – after tests

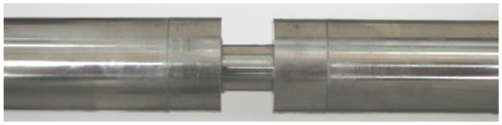

Fig. 7. Compression test sample placed between the test bars

After tests the registered data was subject to further processing in order to achieve stress-strain functions, yield stress and failure strain values.

On the basis of signals, received from the test bars, the strain, stress and strain rate in the sample were calculated, following dependence for elastic bars system:

$$\varepsilon(t) = -2\frac{C_o}{L}\int_0^t \varepsilon_R(t)d\tau \tag{1}$$

$$\sigma(t) = 2\frac{ES_{po}}{S_{pr}}\varepsilon_T(t) \tag{2}$$

$$\dot{\varepsilon}(t) = -2\frac{C_o}{L}\varepsilon_R(t) \tag{3}$$

where: C_o – velocity of elastic wave propagation in the initiating bar, L – sample length, E – Young modulus, S_{po} – cross-section area of the receiving bar, S_{pr} – cross-section area of the sample, $\varepsilon_R(t)$ – signal in time for reflected wave, $\varepsilon_T(t)$ – signal in time for wave in the receiving bar.

Calculated values $\varepsilon(t)$ and $\sigma(t)$ allowed to draw the stress-strain dependence curve for the determined strain rate. Results of the projectile core compression tests, both static and at high strain rates, are shown in Table 1.

Table 1. Results of the projectile cores compression tests: static and at high strain rates

Sample no.	Static compression				Dynamic compression	
	Young's modulus, E [GPa]	Poisson ratio, ν	Ultimate strength, R_m [GPa]	Failure strain, ε_f [%]	Maximum stress, σ_{maks} [GPa]	Plastic strain, ε_{pl} [%]
1	193.4	0.281	4.57	23.2	6.98	5.58
2	190.2	0.272	4.46	16.2	6.74	5.51
3	181.7	0.273	4.76	19.1	6.36	5.55
4	193.0	0.271	4.18	24.0	6.94	5.59
5	190.2	0.257	4.20	17.6	7.09	5.52
Average	189.7	0.271	4.434	20.0	6.82	5.55
Deviation	4.7	0.009	0.24	3.4	0.28	0.04

Example diagrams of the projectile core compression tests, both static and at high strain rates, are shown in Figure 8.

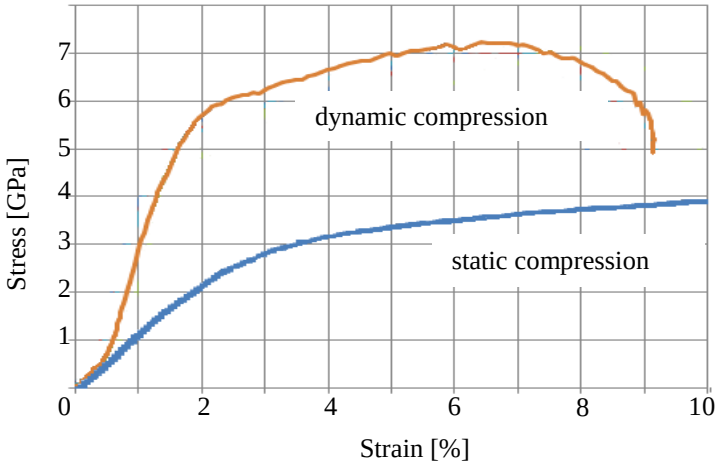

Fig. 8. Stress in function of strain for the compression test of projectile core

After Armox 500T *DP* tests, deformations of the plates were measured in the areas of which the projectile impacted the plate (Fig. 9).

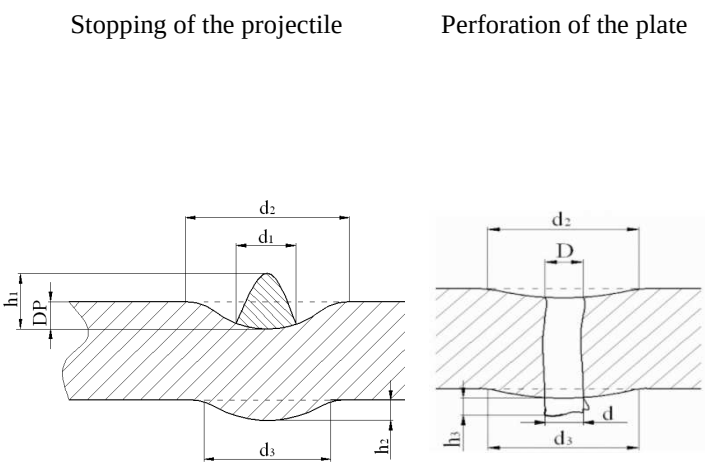

Fig. 9. The Armox 500T plate after the projectile impact: *DP* – depth of penetration/dinge, h_1 – height of hill, d_1 – diameter of hill, d_2 – diameter of dinge, d_3 – diameter of bulge of the back side of the plate, h_2 – height of bulge of the back side of the plate, h_3 – height of the back side of the plate torn off, D – diameter of inlet crater of the perforated plate, d – diameter of outlet crater of the perforated plate

The deformations of the Armox 500T plates measured after projectile impact are shown in Table 2.

Table 2. Results of measured deformations of the Armox 500T plates after the projectile impact

Plate no.	Deformations of the Armox 500T plates							
	Depth of penetration, *DP* [mm]	Diameter of dinge, d_2 [mm]	Height of hill, h_1 [mm]	Height of bulge, h_2 [mm]	Diameter of bulge, d_3 [mm]	Height of the plate back side torn off, h_3 [mm]	Diameter of inlet crater, *D* [mm]	Diameter of outlet crater, *d* [mm]
1	-	-	-	-	33.3	3.8	18.2	17.0
2	-	-	1.1	4.2	38.7	4.2	12.4	-
3	2.2	23.8	-	1.4	23.1	-	-	-

a b c d e f

Fig. 10. The Armox 500T plates after firing:
a – plate 1 front, b – plate 1 back, c – plate 2 front, d – plate 2 back,
e – plate 3 front, f – plate 3 back

4. BUILDING OF NUMERICAL MODELS OF PROJECTILES

The described tests were carried out in order to determine values of the material parameters of the J–C strength model equation, as [1, 2]:

$$\bar{\sigma} = [A + B(\bar{\varepsilon})^n]\left[1 + Cln\left(\frac{\dot{\varepsilon}}{\dot{\varepsilon}_0}\right)\right]\left[1 - \left(\frac{T - T_0}{T_m - T_0}\right)^m\right] \tag{4}$$

where: A – yield stress at ambient temperature, B – hardening constant, $\bar{\varepsilon}$ – effective plastic strain, n – hardening exponent, C – strain rate constant, $\dot{\varepsilon}$ – strain rate, $\dot{\varepsilon}_0$– reference strain rate, T – temperature of the tested material, T_0 – ambient temperature, T_m – melting temperature, m – thermal softening parameter.

From the static compression test results the average stress-strain diagrams were drawn to determine the J–C equation parameter values. In the first instance, the A parameter value was determined from the diagrams, then the B and n parameters were determined, with the use of the fitting curve method, for the data describing plastic range of the diagram.

For tests at high strain rates the average strain rate was specified and then, based on the average compression test diagrams, the parameter C of the J–C equation was determined with the use of the fitting curve method. The determined values of the J–C equation parameters are shown in Table 3.

Table 3. Values of the J–C strength model parameters for the projectile materials

Element	Material	*A* [MPa]	*B* [MPa]	*n*	*C*	*m*	Reference
Projectile core	Steel N12e	1580	2905	0.117	0.075	1.17	Own research
Projectile jacket	Steel 4340	792	510	0.26	0.014	1.03	[2]
Projectile can	Lead	24	300	1	0.1	1.0	[6]
Plate	Armox 500T	1470	702	0.199	0.00549	0.81	[4]

For determining parameter values, simulations of mechanical tests were performed to determine values of the N12e steel failure model parameters. As the material failure model the J–C equation was adopted:

$$\varepsilon_f = \left[D_1 + D_2 e^{D_3 \sigma^*}\right][1 + D_4 ln\dot{\varepsilon}^*][1 + D_5 \left(\frac{T - T_0}{T_m - T_0}\right)] \tag{5}$$

where: $D_1 \div D_5$ – failure parameters, $\dot{\varepsilon}^*$ – dimensionless effective strain rate, σ^* – dimensionless coefficient of pressure to stress relation, T – temperature of the tested material, T_0 – ambient temperature, T_m – melting temperature.

The cylindrical sample in the static compression simulations was made of 43408 four-nodal tetragonal solid elements of 0.5 mm size, and in compression at high strain rates simulations of 287578 such elements. In simulations of the Armox 500T plates penetration, the 12.7 mm type B-32 projectile was made of 52261 four-nodal tetragonal solid elements of 1 mm size, while the armour – of 188538 eight-nodal hexagonal solid elements of 0.75 mm size. In order to reduce the time of calculation only the $50 \times 50 \times 10$ mm size fragments of the three Armox 500T plate were modelled. Adopted coefficients of friction between the materials from which the elements of simulations were made are shown in Table 4.

Table 4. Values of coefficient of friction between the elements of simulations

Type of contact	Static friction coefficient	Dynamic friction coefficient
Steel-steel	0.8	0.8
Steel-lead	0.95	0.95

Correctness of the adopted J–C model parameters values were evaluated by a comparison of the strain character, and also the stress and strain values, obtained in samples during tests and simulations (Fig. 11). Only the parameters $D_1 \div D_3$ of the J–C failure model having the biggest influence on the failure strain value were determined [3]. The J–C failure model has a status of instantaneous failure model, that means that after the element damage (a part) its stiffness and strength is removed automatically. The failure occurs when the parameter *D* achieves value 1:

$$D = \sum \frac{\Delta \bar{\varepsilon}^{p}}{\varepsilon_f} = 1 \tag{6}$$

where: $\Delta\bar{\varepsilon}^{p}$ – increment of the effective plastic strain, ε_f – failure strain.

Because of lack of necessary data (only compression tests for unnotched samples were made) the values of the failure model parameters $D_1 \div D_3$ have been obtained arbitrarily. Some initial values of the parameters $D_1 \div D_3$ had been assumed and then these values had been tuned (Table 5) until the smallest differences between simulations and experiments results were obtained. Similarly to the static compression tests, in simulation the sample accumulated stresses of 4 GPa and was damaged after achieving 18% strain. Before the failure, the specific „barrel" shape of the sample occurred, both during the simulation and tests.

In the case of the simulation of tests at high strain rates the sample was not destroyed, and its plastic strain value was ca. 5%. The maximum stress registered in a sample amounted to 7 GPa, similarly to the tests.

Table 5. Values of the J–C failure model parameters for the simulation elements

Element	Material	D_1	D_2	D_3	D_4	D_5	Reference
Projectile core	N12e steel	0.036	0.083	-3.0	0	0	Own research
Projectile jacket	4340 steel	0.05	3.44	-2.12	0.002	0.61	[2]
Plates	Armox 500T	0.068	5.328	-2.554	0	0	[5]

Additional verification of the built numerical models was the simulation of the three coherent Armox 500T plates penetration with the 12.7 mm type B-32 projectile (Fig. 12).

The depth of penetration obtained in the simulation (DP_s = 21 mm) was compared to the depth of penetration obtained in the test (DP_e = 22 mm). The high conformity of results obtained (difference < 5%) confirms that the J–C parameter values were determined correctly.

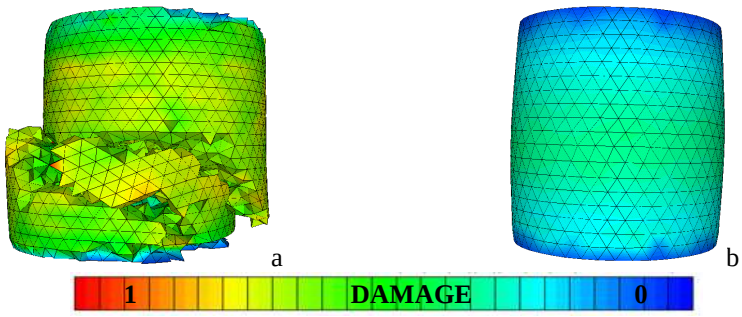

Fig. 11. The N12e steel sample damage map after simulation:
a – static compression, b – compression at high strain rates

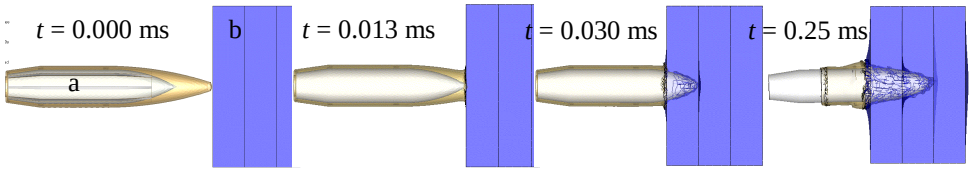

Fig. 12. Simulation of the three coherent Armox 500T plates penetration with the 12.7 mm type B-32 projectile: a – projectile, b – Armox 500T plates (3 × 10 mm)

5. CONCLUSIONS

On the basis of the tests results and the carried out computer simulations the following conclusions have been drawn:

1. The course of the stress-strain curves for the N12e steel samples significantly depends on the strain rate. In the compression tests at high strain rates the samples show a doubling in yield strength (ca. 7 GPa) in relation to the static compression tests (ca. 3.5 GPa).
2. The characteristics and values of parameters obtained from the tests conform to the numerical simulations, what testifies correctness of the adopted values of the Johnson–Cook strength and failure models parameters.
3. The characteristics of the N12e steel samples failure during the static compression tests is very similar to the failure of samples obtained in the simulations. In both cases, the samples were crushed after achieving an 18% strain, cumulating stress equal to 4 GPa.
4. The specific „barrel" shape of the sample before the failure, was clearly visible during both the simulations and tests.
5. The sample was not destroyed and its plastic strain amounted to ca. 5% during both simulations and tests of compression at high strain rates. The maximum stress in samples, registered during simulations, amounted to 7 GPa, similarly to the tests.
6. The depth of penetration of the three coherent Armox 500T steel plates, obtained during simulations (DP_s = 21 mm) is very similar to the test results (DP_e = 22 mm), and the small difference of < 5% confirms, that the Johnson–Cook parameter values were adopted correctly.

This research was carried out within the project *„Technology of production of superhard nano-structural Fe-based alloys and their application in passive and passive-reactive armours”* realized by consortium of Institute for Ferrous Metallurgy in Gliwice (Poland) and Military Institute of Armament Technology in Zielonka (Poland) financially supported by the European Fund for Regional Development in Poland under the contract No. UDA-POIG.01.03.01-00-042/08-00.

REFERENCE

[1] Johnson G.R., Cook W.H., A Constitutive model and data for metals subjected to large strain, high strain rate and high temperature, *Proceedings of the 7th International Symposium on Ballistics*, pp. 541-547, 1983.
[2] Johnson G.R., Cook W.H., Fracture characteristics of three metals subjected to various strains, strain rates, temperatures and pressures, *Engineering Fracture Mechanics*, vol. 21, pp. 31-48, 1985.
[3] Hancock J.W. and Mackenzie A.C., On the Mechanism of Ductile Failure in High-Strength Steels Subjected to Multi-Axial Stress-States, *Journal of the Mechanics and Physics of Solids*, vol. 24, pp. 147-175, 1976.
[4] Nilsson M., *Constitutive model for Armox 500T and Armox 600T at low and medium strain rates*, s. l, Swedish Defence Research Agency, TR FOI-R-1068-SE, 2003.
[5] Skoglund P., Nilsson M., Tjernberg A., Fracture modelling of a high performance armour steel, *Journal de Physique IV*, France, vol. 134, pp. 197-202, 2006.
[6] Børvik T., Dey S., Clausen A.H., Perforation resistance of five different high strength steel plates subjected to small-arms projectiles, *International Journal of Impact Engineering*, vol. 36, pp. 948-964, 2009.